INFLUENCE OF DOPANT TYPES ON THE MORPHOLOGICAL TRANSFORMATION OF GREEN-SYNTHESISED TUNGSTEN TRIOXIDE NANOPARTICLES

[1,3]J.O. Tijani, [1,3] O. Ugochukwu, [1]L.A. Fadipe, [1,3]M.T. Bankole, and [2,3]A.S. Abdulkareem

[1]Department of Chemistry, Federal University of Technology, PMB. 65, Minna, Niger State
[2]Department of Chemical Engineering, Federal University of Technology, PMB.65, Minna, Niger State, Nigeria
[3]Nanotechnology Research Group, Centre for Genetic Engineering and Biotechnology (CGEB), Federal University of Technology, P.M.B 65, Bosso, Minna, Niger State, Nigeria
*Corresponding author: jimohtijani@futminna.edu.ng, +2348057344464

ABSTRACT

WO_3 nanoparticles were synthesized by green method involving the interaction between ammonium paratungstate precursor and aqueous leaves extract of *Spondias mombim*. The effect of calcination temperature and dopant types on the phase types of WO_3 were examined. Subsequently, doping of WO_3 with Boron, Aluminium, Phosphorus and Iodine were achieved via a wet impregnation method to evaluate their influence on the size and shape of WO_3. The characterization was done using HRSEM, BET and XRD The HRSEM micrograph demonstrated morphological transformation from spherical to thin and thick rods, bamboo-bundles and platelet-like structure depending on the dopant type and calcination temperature. The XRD pattern of undoped WO_3 nanoparticles showed the formation of purely monoclinic phase at calcination temperature 550°C while mixed phase were noticed in the samples prepared at other temperatures. The BET analysis showed that as-prepared WO_3 nanoparticles doped with B, Al, I and P possessed higher surface area in the order of B-WO_3 (399.50 m^2/g) > I-WO_3 (392.50 m^2/g) > Al-WO_3 (388.46 m^2/g) > P-WO_3 (356.76 m^2/g) > undoped WO_3 (352.49 m^2/g). The study demonstrated that temperature influenced the morphological characteristics of WO_3 while the four elements played a dual of a dopant as well as structure-directing agent.

Keywords: Biosynthesis, Tungsten Oxide, *Spondias Mombin,* Dopant types, morphological characteristics

INTRODUCTION

Tungsten (IV) oxide also known as tungsten trioxide (WO_3) is an n-type semiconductor photocatalyst that contains oxygen and the transition metal tungsten and have drawn much attention as a functional oxide for various types technological application due to their moderate band gap and high electric resistivity [1]. Amongst the polymorphs of WO_3, that have attracted attention are the hexagonal (h-WO_3) and the monoclinic (m-WO_3). The addition of trace impurities of metal and non-metals have been reported to alter the morphological characteristics and band gap of the WO_3 nanoparticles thereby enhancing its photocatalytic performance [2]. Doping of WO_3 with metals, metalloids and non-metals have been found as a feasible alternative to modify WO_3 nanostructure for better performance under visible light. In

this study, boron, aluminium, phosphorus and iodine were selected as dopant in the synthesize of WO_3 due to their availability and tendency to replace oxygen and reduce the band gap energy of WO_3 [3]. WO_3 nanoparticles were routinely synthesized by various physical and chemical methods such as solvothermal-reduction, hydrothermal technique, sol-gel technique, non-sputtering and electrochemical technique, catalytic chemical vapour deposition, photodeposition, to mention but a few [4] However, these methods are costly, toxic, require complex synthesis procedure, pressure and high energy requirement. Conversely, Green synthesis involving the use of plant extracts to prepare nanoparticles have several advantages such as availability of the plant material, environmental beningn nature and as well as broad presence of metabolites (the phytochemicals) compared to other methods [5]. These constituents are responsible for the reduction of metals from their respective oxidation state to zero valence state. In this study, green synthesis of WO_3 nanoparticle based on the utilization of aqueous leave extract of *Spondias mombim*. was be explored. The effect of calcination temperatures on morphological characteristics of WO_3 nanoparticle was investigated. Separate incorporation of different amount Boron, Aluminium, Phosphorus and Iodine onto the lattice layer of WO_3 nanoparticles was also carried out. The prepared WO_3 nanoparticles, B-WO_3, Al-WO_3, P-WO_3 and I-WO_3 nanocomposites were characterized.

2.0 MATERIALS AND METHODS

Materials

Ammonium tungsten hydrate, Aluminium oxide, Boric acid, Ammonium phosphate, Ammonium Iodine were supplied by Sigma Aldrich and used without any further purification. Fresh leaves of *Spondias mombin* (Plum Hog) were randomly collected from Bida, Niger State, washed, sun dried in the open air for a week, and crushed to a fine powder using a mechanical blender.

Green Synthesis of undoped and mono doped WO_3 nanoparticles

About one hundred grams (10 g) of the dried leaves powder of *Spondias mombin* was mixed with 50 mL of distilled water and extracted under reflux condition at 80^0C. After 2 hours, the aqueous leaf extract was obtained by filtration. 90 mL of 0.06 M of tungsten precursor was mixed with 10 mL of leaf extracts. The pH of the mixture was not adjusted however stirred on a magnetic stirrer with a stirring speed of 500 rpm at 80°C for 3 hours. The WO_3 nanoparticle was centrifuged and washed severally with distilled water. The separated sample was oven dried at 100°C for 3 hours and further calcined at different temperatures of 450°C, 550°C, 650°C and 750°C for 2 hours in muffle furnace. For the preparation of B-doped WO_3, Al doped-WO_3 P-doped WO_3 and I-doped WO_3, nanoparticles; 20 mL each of 0.1 M Boric acid, Aluminium oxide, Ammonium phosphate and Ammonium Iodide was mixed with 2.5 g of the prepared WO_3 and stirred on a magnetic stirrer at 500 rpm for 3 hours followed by centrifugation at 1000 rpm for 15 minutes and thereafter the residue washed with distilled water. Separated sample was oven dried at 100°C for 3 hours and calcined at the optimum temperature of 550°C in furnace for 2 hours.

Characterization of the prepared nanomaterials

The prepared nanomaterials were characterized for their morphologies, phase structures and surface areas using High Resolution Scanning Electron Microscope Zeiss Auriga, X-ray diffraction AXS Bruker D8 and Brunauer Emmett Teller N_2 adsorption-desorption NOVA 2400e

3.0. RESULTS AND DISCUSSION

- **HRSEM and XRD analysis of WO_3 nanoparticles synthesised at different temperatures**

The possible morphological transformation of the synthesized WO_3 at different calcination temperatures were examined using HRSEM and the micrographs obtained are shown in Figure 1. XRD analysis was done to investigate the phase nature of the synthesized materials at different temperatures.

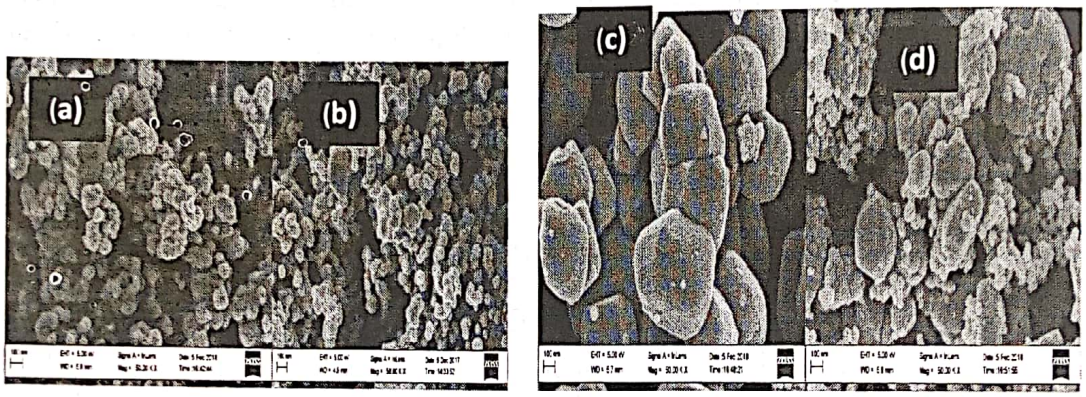

Figure 1: HRSEM micrograph of WO_3 nanoparticles synthesised at (a) 450°C (b) 550°C (c) 650°C(d) 750°C

It can be observed from Figure 1(a) (the HRSEM-images of WO_3 nanoparticles calcined at 450^0C) that the nanoparticles were highly dispersed, agglomerated and spherical in shape which correspond to the monoclinic phase of WO_3 with average particle size of 29.5 nm. For WO_3 nanoparticle calcined at 550°C, distributed less agglomerated spherical shape were formed which depict monoclinic polymorphs of WO_3 with average particle size of 27.8 nm. The formation of less agglomerated spherical shape at 550°C may be ascribed to the effect on the interfacial energy growth rate coefficient and solubility solution media which increase nucleation of the nanocluster and more growth in the host of WO_3. In the case of WO_3 nanoparticles calcined at 650°C, closely packed, dense and purehexagonal shape were formed with average particle size of 18.7 nm. The formation of pure hexagonal phase at 650°C was linked to reduction of dielectric constant and electrostatic repulsion among highly charged W^{6+} ions which later became stronger and created more and formed open structures as hexagonal [4]. At 750°C, mixtures of less agglomerated hexagonal and spherical shape were observed with average particle size 33.4 nm. The formation of mixed shapes at higher calcination temperature may be attributed to sintering of WO_3

nanocrystals at higher temperature. This implies that temperature increment causes morphological changes from spherical to hexagonal shape [5].

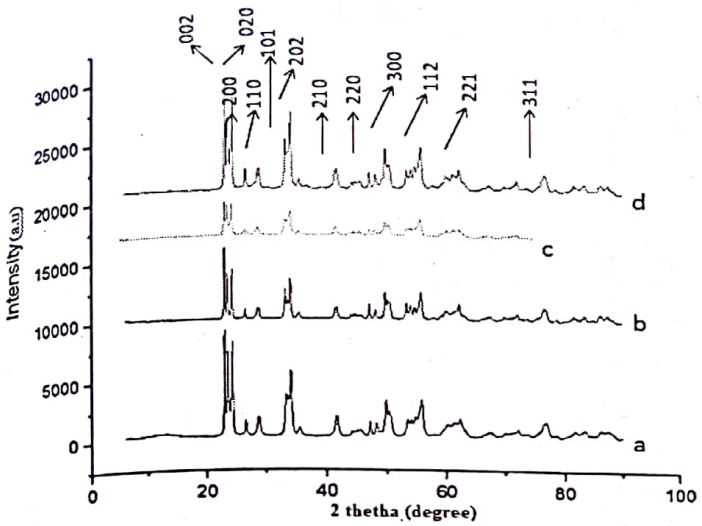

Figure 2: XRD pattern of WO_3 prepared at different temperatures (a) 450^0C (b) 550^0C (c) 650^0C (d) 750^0C

At 450°C (fig 2 (a)), sharp and intense peaks with crystal planes (002), (020), (200) and (202) were observed at bragg angle 2 thetha value of 23.13°, 24.00°, 24.56° and 28.12° respectively, which correspond to monoclinic phase of WO_3 and the average crystalline size was calculated to be 18.3 nm according to Debye Scherrer equation [6]. Similar, trend was observed for WO_3 nanoparticle calcined at 550°C with an average particle size of 17.3 nm. The XRD pattern of WO_3 nanoparticle produced at 650°C revealed characteristic strong but small peaks at 2 thetha values of 23.13°, 24.00°, 24.56°, 28.12°, 14.59°, 28.14°, 28.59° and 45.00° which correspond to the following crystal planes of (002), (020), (200), (110), (101), (202), (101) and (112) respectively. These peaks matched with the pattern of hexagonal phase of WO_3 and have average crystalline size of 12.3 nm. The XRD pattern observed at 750°C revealed sharp peaks which correspond to (100), (002), (020), (110), (101), (202), (220), (112) and (221) crystal plane at bragg angle 2 thetha value of 14.59°, 23.13°, 24.00°, 28.14°, 28.59°, 28.12°, 34.20°, 42.00° and 50.01°. These peaks match properly with monoclinic and hexagonal phase of WO_3 and have average crystalline size of 18.9 nm. It should be mentioned that pure phase of monoclinic WO_3 were formed at 450°C and 550°C formed with average crystalline size of 17.3 nm and 18.32 nm respectively with the latter having smaller size of (17.3 nm) than the former (18.2 nm) This means that the optimum temperature to synthesis pure monoclinic phase of WO_3 nanoparticle based on size is 550°C.

HRSEM analysis of bare and doped WO_3 nanoparticles with different elements

Figure 3 represents the morphology of the prepared WO_3 nanoparticles doped with different elements

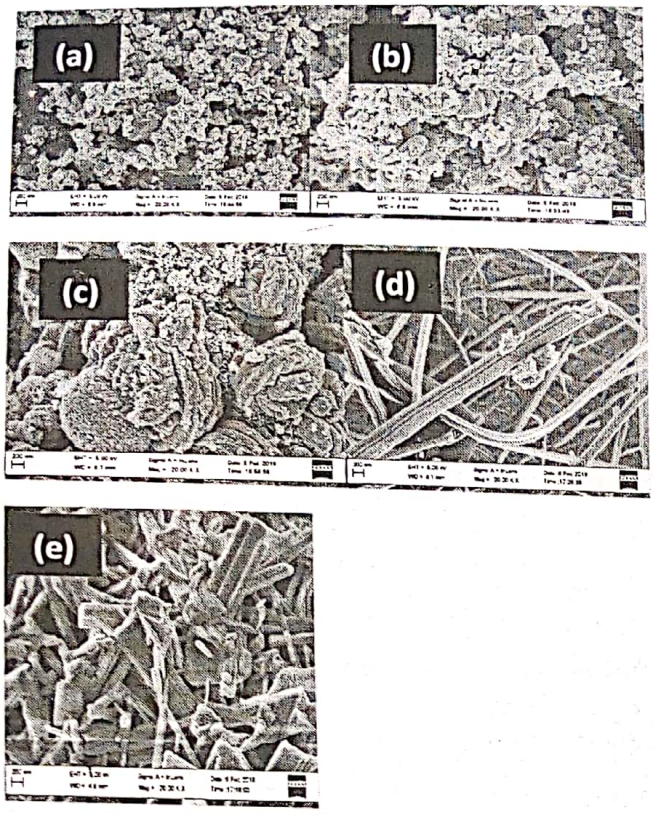

Figure 3: HRSEM micrograph of (a) undoped WO_3 (b) Boron (c) Aluminium (d) Phopshorus (e) Iodine doped WO_3 nanoparticles

As shown in Figure 3, less aggregated and well distinct spherical of WO_3 produced. When Boron was mixed with WO_3, highly compacted disc-like and hexagonal nanostructures were observed. For Aluminium doped WO_3, plate or ring like morphology compared to spherical shape (undoped WO_3) was noticed. In the case of P-WO_3, long and thick bamboo-like morphology were formed while short and long rod-like symmetry was formed for Iodine doped WO_3. It is obvious that addition of different elements largely influenced the morphology of WO_3 nanoparticles. The difference may be attributed to the nature of the dopant vis-a-viz, ionic size and atomic weight [6]. It appears that as these elements acted as a structure directing agent [2,4].

BET Analysis of Undoped and mono doped WO_3 Nanoparticles

The surface area of each prepared catalyst is given in Table 1.

Table 1. Specific surface area and pore volume of undoped and mono doped WO_3 nanoparticles

Samples	BET surface area (m^2/g)	Pore volume (m^2/g)
Bare WO_3	352.49	2.13
B-WO_3	392.50	1.99
Al-WO_3	366.76	2.10
P-WO_3	356.76	2.14
I-WO_3	382.25	2.10

From Table 1, it is obvious that the surface area of the as-synthesized WO_3 nanoparticles differ and increase slightly or significantly depending on the nature of the dopants. The increase in surface area could be ascribed to the morphological transformation of the spherically shaped WO_3 nanoparticle to ring/plate or rod-like shaped nanocomposites caused by the substitutional effects of the dopants with either W or O atom [7].

CONCLUSION

WO_3 nanoparticles were successfully synthesized by biosynthetic route involving *Spondias mombin* plant extract. The HRSEM/XRD/BET results demonstrated that the morphological transformation and surface area of WO_3 nanoparticles are largely dependent on the applied calcination temperature and the incorporated elements.

REFERENCES

1. N. Prabhu, S. Agilan, N. Muthukumarasamy, and T.S. Senthil (2014). Preparation and Characterizations of Copper doped WO_3 Nanoparticles Prepared by Solvo Thermal cum Chemical method. International Journal of Chemical Technology Research, 6(7): 3487-3490.

2. S.A. Xiaobo (2014). Effect of doping metal oxide nanoparticles. Journal of Royal Society of Chemistry, 4 (8): 386 – 402.

3. J. Zhang, K. Tse, M. Wong, Y. Zhang, and Y. Zhu (2016). Mechanism of Doping Nanomaterial. Journal of Frontiers of Physics, 11(2): 23-28

4. N.S. Kavitha, K.S. Venkatesh, N.S. Palani, and R. Ilangovan (2017). Fungus mediated biosynthesis of WO_3 nanoparticles using *Fusarium solani* extract. American Institute of Physics, Conference Proceedings, 1832, 050130; Doi: 10.1063/1.4980363

5. X. Hu, P. Xu, H. Gong, and G. Yin (2018). Synthesis and Characterization of WO_3/Graphene nanocomposites for enhanced photocatalysts activities by one-step in situ hydrothermal reaction. International Journal of Material Science, 11 (2): 142-154.

6. C. J. Hung, H.Y. Huang, C.H. Chen, P. Lin, and Y.T. Tseng (2014). Hydrothermal formation of tungsten trioxide network on seed free substrate and their properties in electrochromic device. Transaction on Component Packaging and Manufacturing Technology Journal, 4(1): 1-12

7. N.K. Hang, N.A. Jaffar, L.L. Minggu, and M.B. Kassim (2016). Fabrication and characterization of Fe-doped tungsten trioxide photoelectrode in aqueous medium using tungstic acid and ferrocene as starting materials. Malaysian Journal of Analytical Science, 20(4): 923-930